Flexibility capacity approximation and aggregation for microgrid control application ⋆

Niels Thobie, Nabil Sadou, Hervé Guéguen

Flexibility capacity approximation and aggregation for microgrid control application ⋆

Niels Thobie * **Nabil Sadou** * **Hervé Guéguen** *

* *IETR - Centralesupelec, Rennes, France*
(firstname.lastname@centralesupelec.fr)

Abstract: With the electrification of our uses and the massive integration of intermittent renewable production sources, demand-side flexibility is a way to maintain balance between production and consumption. This paper presents an individual flexibility capacity approximation that ensure confidentiality and low communication effort. This method is derived from the homothetic approximation technique. Our method is compared to other methods through a microgrid control problem. The results show that it provides a good tradeoff between fidelity and computation time, which makes it efficient for a massive group of buildings.

Keywords: Microgrid Control, Flexibility Approximation and Aggregation, Demand Response Flexibility.

1. INTRODUCTION

Energy transitions development offers a diversity of energy sources. The renewable energy sources (RES) are increasingly integrated into the different power grids. The production periods of those sources may not face the consumption period of our uses, creating different issues in the grids. In the case of Microgrids (MG), a small and local power grid that can be autonomous from the global grid or connected to it, the problematic of self-consumption is important to provide the needed energy or, on the other hand, avoid the potential spillage of energy to promote the integration of RES.

With the development of automated systems in building electrical uses, a solution is to offer flexibility through demand response (DR) schemes. Flexibility can come from the power supply sources, the storage units, or the load demand. There are different strategies from the demand-side management (DSM) such as load shifting, peak shaving, or valley filling (Lund et al., 2015). One of the definitions of flexibility is a system's capacity to shift its power consumption in time to balance the supply and demand in order to consume affordable and low-carbon electricity.

In the literature, demand-side flexibility is considered through different sources of flexibility, such as thermostatically controlled loads (TCL) (Zhao et al., 2017), electric vehicles (EV) (Essayeh and Morstyn, 2023) or battery (BT) (Öztürk et al., 2022). The flexibility can also be modeled as a flexibility envelope (Zhang and Guéguen, 2022) or ramps (Saavedra et al., 2022) where the load can fluctuate dynamically.

A model explored in the literature to describe the dynamic aspect of individual flexibility capacity is the polytopial approach described through a set of linear constraints (Zhao et al., 2017; Zhang and Guéguen, 2024). Those flexibility polytopes compute the set of all power profiles by which the household's demand profile can differ from the default demand profile of no flexibility (Öztürk et al., 2022).

With a large number of households, a step of aggregation can be needed. This step reduces the utility's optimization complexity and communication effort, as only aggregated variables are concerned for the energy management system (EMS) linked to the households (Öztürk et al., 2022). However, we need to guarantee confidentiality before sending information such as the individual flexibility capacity to the EMS. Also, with polytopes, the aggregation is made through Minkowski sum (MS), which is an NP-complex problem. To solve this problem, some papers developed methods of approximation of the MS to limit the complexity of this step, but those methods need a specific convex envelope to operate the aggregation step. Therefore, to guarantee confidentiality and approximate the step of approximation, an individual approximation is needed.

There exists different methods that approximate the MS using approximation of polytopes, which imply different shapes of convex envelopes, such as battery homothet (Zhao et al., 2017), virtual battery (Zhang and Guéguen, 2024), zonotopes (Müller et al., 2019), cuboid homothet (Nazir et al., 2018) or ellipsoid (Barot, 2017). (Öztürk et al., 2022) compare different methods that approximate the MS through different quality criteria (computation time, fidelity criterion. . .), classified into two approaches: inner approximations and outer approximations.

Through the literature analysis, two methods reveal interesting features: the virtual battery approximation method

⋆ This work benefited from state aid managed by the Agence Nationale de la Recherche (ANR) under the "France 2030" programme, bearing the reference ANR-22-PETA-0009 (FlexTASE project, in the framework of PEPR TASE).

(Zhang and Guéguen, 2024) for fidelity (defined as the efficiency of the approximation to transmit the maximum information from the original polytope) and the homothet battery approximation method (Zhao et al., 2017) for computational time efficiency. The issue of the first method is that the approximation is made through non-linear optimization problems, which implies no guarantee of convergence. The second method is really efficient for MS approximation, but the same prototype is needed for each individual approximation. However, due to the variation in the flexibility capacity polytope in terms based on the variation of thermal characteristics and thermal routine, the choice of prototype is limited, and the approximation can be poor in terms of the transcript of individual flexibility.

This paper presents a novel method for approximating and aggregating individual flexibility capacity. The approach achieves a compromise between model fidelity and computational efficiency, a key aspect in microgrid control applications. This paper is organized as follows: first, the individual flexibility capacity is estimated as a polytope. The considered flexibility source is the heating. After, an approximation method of the individual flexibility capacity and the aggregated flexibility capacity is presented. Following this, our method is implemented in a microgrid control problem. A use case is presented, and the results are discussed. A conclusion on the proposed method is developed at the end of the paper, with a perspective on future works.

2. METHODOLOGY

2.1 Individual Flexibility capacity

As stated in the introduction, the considered flexibility source is the heating. So, for each building i, a commonly-used state-space thermal model is used (Boodi et al., 2022) for the thermal dynamics of the building, such as :

$$\begin{aligned} x(k+1) &= A_i x(k) + B_{u,i} u(k) + B_{d,i} \theta_{ext}(k) \\ y(k) &= C_i x(k) \end{aligned} \tag{1}$$

Where $x = (\theta_{th}\ \theta_w)^T \in \mathbb{R}^2$ is the thermal state of the building and θ_{th} and θ_w are respectively the inner temperature and the wall temperature of the building, u the power from the heating and θ_{ext} the disturbance, which is the outside temperature, y the inner temperature of the building, A_i, $B_{u,i}$, $B_{d,i}$ and C_i are matrices with the correct dimensions.

By using Model Predictive Control (MPC) (Zhang and Guéguen, 2022), the baseline $\mathbf{u}_{bs}(k) = \{u_{bs}(k)\}_{k\in\mathcal{N}}$ is generated such as the power profile that minimizes the cost of the heating and maintains the inner temperature within a comfortable temperature range, such as :

$$\underline{\theta}^n_{th}(k+1) \leq \theta_{th}(k+1) \leq \overline{\theta}^n_{th}(k+1) \tag{2}$$

Where $\underline{\theta}^n_{th}$ and $\overline{\theta}^n_{th}$ are respectively the minimum and maximum inner comfort temperatures. By introducing flexibility, the building is able to modulate its consumption to make upward or downward flexibility :

$$u(k) = u_{bs}(k) + u_f(k) \tag{3}$$

Where u_f described the flexibility power. To implement the flexibility, the range of temperature must be enlarged outside the comfort range, such as :

$$\underline{\theta}_{th}(k+1) \leq \underline{\theta}^n_{th}(k+1) \leq \theta_{th}(k+1) \leq \overline{\theta}^n_{th}(k+1) \leq \overline{\theta}_{th}(k+1) \tag{4}$$

Where $\underline{\theta}_{th}$ and $\overline{\theta}_{th}$ are respectively the enlarged lower and upper bounds of inner temperature. An example of the temperature trajectory generated with MPC with the comfort range and the enlarged comfort range is presented in figure 1. To model the capacity of flexibility of a building

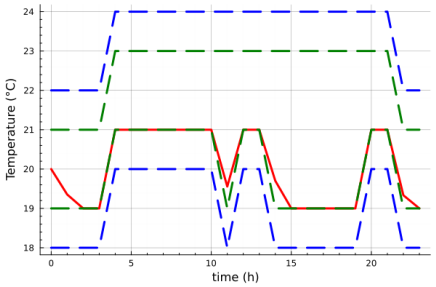

Fig. 1. Temperature trajectory generated through MPC (red), comfort temperature range (green), enlarged temperature range (blue)

i, all the trajectories of consumption that derivate from the baseline are computed in sets of linear equations for a defined flexibility horizon N_f. The following polytope is obtained :

$$\mathcal{P}^{rl}_i := \left\{ u_f \in \mathbb{R}^{N_f} \;\middle|\; \begin{array}{c} x(k+1) = A_i x(k) + B_{u,i}(u_{bs}(k) \\ +u_f(k)) + B_{d,i}\theta_{ext}(k) \\ y(k) = C_i x(k) \\ \underline{u}(k) \leq u_{bs}(k) + u_f(k) \leq \overline{u}(k) \\ \underline{\theta}_{th}(k+1) \leq y(k+1) \leq \overline{\theta}_{th}(k+1) \end{array} \right\} \tag{5}$$

With $\underline{u}$ and $\overline{u}$ respectively the lower and upper bounds of heating. The equation (5) can be rewritten as :

$$\mathcal{P}^{rl}_i := \left\{ u_f \in \mathbb{R}^{N_f} \;\middle|\; H^{rl}_i u_f \leq d^{rl}_i \right\} \tag{6}$$

Where $H^{rl}_i \in \mathbb{R}^{4N_f \times N_f}$ and $d^{rl}_i \in \mathbb{R}^{4N_f}$. The matrices described the linear equations that characterize every derivation of the baseline. An example of the capacity polytope is given in figure 2.

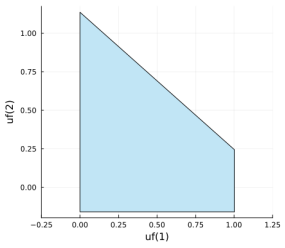

Fig. 2. Example of capacity polytope $\mathcal{P}^{rl}_i$ for $N_f = 2$

2.2 Flexibility approximation

The building owners may regard their actual capacities as confidential and might be reluctant to share them. So, to ensure privacy protection and to facilitate the aggregation step, an approximation process of the capacity polytope is implemented. However, the needed approximation method has to be performant in terms of fidelity and computation time in order to be implemented in a control and sizing optimization problem.

As discussed in the introduction, homothet battery approximation is efficient in terms of computation time, but the fidelity depends on the choice of prototype. Also, the virtual battery approximation is effective in terms of fidelity, but the implementation is made through a non-linear problem. One proposition would be using the virtual battery model as a prototype. An example is shown in figure 3.

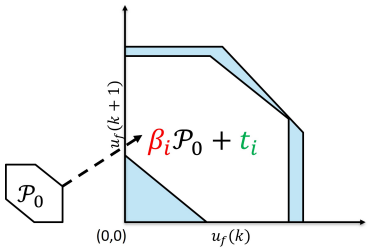

Fig. 3. Example of flexibility capacity (light blue) and approximation made through virtual battery prototype $\mathcal{P}_0$ scaled and translated through factors β_i and t_i for $N_f = 2$

In this example, the (0,0) point is the "*no-flexibility*" point. It is in the bottom-left corner of the polytope, which means that we can only offer upward flexibility or no flexibility. However, the optimal homothet approximation doesn't include the "*no-flexibility*" point. This solution can't be acceptable, as the flexibility capacity of the building must include the "*no-flexibility*" point. Therefore, the virtual battery prototype can't be used. An equivalent situation can happen if we can only offer downward flexibility or no flexibility. As the homothet approximation with a virtual battery prototype can't be used, another method is proposed to avoid those extreme cases. The proposition of this paper is to divide the problem into two approximations : the power-only flexibility capacity approximation and the thermal-only flexibility capacity approximation. Therefore, the flexibility capacity polytope can be written as the intersection of two polytopes, such as :

$$\mathcal{P}_i^{rl} = \mathcal{P}_i^{rl,pw} \cap \mathcal{P}_i^{rl,th} \tag{7}$$

Where $\mathcal{P}_i^{rl,pw}$ and $\mathcal{P}_i^{rl,th}$ are respectively the flexibility capacity polytope of the power constraints only $(\underline{u}(k) \leq u_{bs}(k) + u_f(k) \leq \overline{u}(k))$ and the thermal constraints only $\left(\underline{\theta}_{th}(k+1) \leq y(k+1) \leq \overline{\theta}_{th}(k+1)\right)$. An example is given in figure 4.

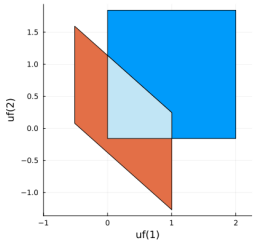

Fig. 4. Flexibility capacity polytope $\mathcal{P}_i^{rl}$ (light blue) as the intersection of $\mathcal{P}_i^{rl,pw}$ (blue) and $\mathcal{P}_i^{rl,th}$ (orange)

Power constraints polytope approximation The power constraints polytope $\mathcal{P}^{rl,pw}$ is expressed in H-polytopic form as follows :

$$\mathcal{P}_i^{rl,pw} = \left\{u_f \in \mathbb{R}^{N_f} | H_i^{rl,pw} u_f \leq d_i^{rl,pw}\right\} \tag{8}$$

With $H_i^{rl} = [-I_{N_f}\ I_{N_f}]$, I_{N_f} the identity matrix of size N_f and $d_i^{rl} \in \mathbb{R}^{2N_f}$. This polytope is defined through direct equations on u_f, but an approximation step is made to simplify the aggregation step. We want to approximate the flexibility capacity polytope by $\mathcal{P}_i^{ap,pw}$ expressed as :

$$\mathcal{P}_i^{ap,pw} = \{u_f \in \mathbb{R}^{N_f} | H_i^{rl,pw} u_f \leq \alpha \cdot d_i^{rl,pw}\} \tag{9}$$

Where :

$$\alpha = \begin{bmatrix}\alpha_1 & \alpha_2 & \dots & \alpha_{2N_f}\end{bmatrix}, \alpha_n \in [0;1] \quad \forall n \in [\![1; 2N_f]\!] \tag{10}$$

We need to find the smallest polytope $\mathcal{P}_i^{ap,pw}$ such that $\mathcal{P}_i^{rl}$ is included in $\mathcal{P}_i^{ap,pw}$. Therefore, we need to find the smallest vector α, where each element α_n satisfy the containment constraint in any direction of the polytope. This can be reformulated :

$$\begin{aligned} \min_{\alpha_n} \quad & \alpha_n \quad \forall n \in [\![1; 2N_f]\!] \\ \text{s.t.} \quad & \mathcal{P}_i^{rl} \subset \mathcal{P}_i^{ap,pw} \end{aligned} \tag{11}$$

This problem (11) can be resolve using Farkas lemnas :

$$\begin{aligned} \min_{\alpha_n, G} \quad & \alpha_n \quad \forall n \in [\![1; 2N_f]\!] \\ \text{s.t.} \quad & GH_i^{rl} = H_i^{rl,pw} \\ & Gd_i^{rl} \leq \alpha \cdot d_i^{rl,pw} \\ & G_{ij} \geq 0 \quad \forall i,j \in dim(G) \quad , \alpha_n \in [0;1] \end{aligned} \tag{12}$$

As the optimal vector α^* is found, the approximation polytope $\mathcal{P}^{ap,pw}$ can be written such as :

$$\begin{aligned} \mathcal{P}_i^{ap,pw} &= \{u_f \in \mathbb{R}^{N_f} | H_i^{rl,pw} u_f \leq d_i^{ap,pw}\} \\ d_i^{ap,pw} &= \alpha^* \odot d_i^{rl,pw} \end{aligned} \tag{13}$$

With $\odot$ the term-to-term multiplication symbol. The resultant approximated polytope will be useful for the step of thermal constraints polytope approximation.

Thermal constraints polytope approximation To approximate the thermal constraints-only polytope, we expressed $\mathcal{P}_i^{rl,th}$ in H-polytopic form such as :

$$\mathcal{P}_i^{rl,th} = \{u_f \in \mathbb{R}^{N_f} | H_i^{rl,th} u_f \leq d_i^{rl,th}\} \tag{14}$$

Where :

$$H_i^{rl,th} = [-M; M] \in \mathbb{R}^{2N_f \times N_f}, d_i^{rl,th} \in \mathbb{R}^{2N_f} \tag{15}$$

$$M = \begin{pmatrix} C_i B_{u,i} & 0 & \dots & 0 \\ C_i A_i B_{u,i} & C_i B_{u,i} & \ddots & \vdots \\ \vdots & \vdots & \ddots & 0 \\ C_i A_i^{Nf-1} B_{u,i} & C_i A_i^{Nf-2} B_{u,i} & \dots & C_i B_{u,i} \end{pmatrix} \tag{16}$$

However, the approximation step will not be made directly on this polytope. A limitation step will be added to search only on the feasible power domain. To do this, we normalize the polytope such as :

$$\begin{aligned} \mathcal{P}_i^{rl,th} &= \{u_f \in \mathbb{R}^{N_f} | \hat{H}_i^{rl,th} u_f \leq \hat{d}_i^{rl,th}\} \\ \hat{H}_i^{rl,th} &= \{\hat{h}_j\}_{j=1}^{2N_f} \in \mathbb{R}^{2N_f \times N_f}, \hat{h}_j = \frac{h_j}{\|h_j\|} \\ \hat{d}_i^{rl,th} &= \{\hat{d}_j\}_{j=1}^{2N_f} \in \mathbb{R}^{2N_f}, \hat{d}_j = \frac{d_j}{\|h_j\|} \end{aligned} \tag{17}$$

Where h_j and d_j are, respectively, the line j of $H_i^{rl,th}$ and $d_i^{rl,th}$. By doing this, we have constraints of the same form as the power-constraint polytope $\mathcal{P}_i^{rl,pw}$ for the first and the $N_f + 1$ constraints. Therefore, the limitation is expressed such as :

$$\begin{aligned} \hat{d}_{i,1}^{rl,th} &= \min(\hat{d}_{i,1}^{rl,th}, d_{i,1}^{ap,pw}) \\ \hat{d}_{i,N_f+1}^{rl,th} &= \min(\hat{d}_{i,N_f+1}^{rl,th}, d_{i,N_f+1}^{ap,pw}) \end{aligned} \tag{18}$$

Now that the limitation step is made, we can approximate the polytope $\mathcal{P}_i^{rl,th}$. We use the inner homothet approximation (Zhao et al., 2017). From this approximation, a scaling factor β_i and a translation factor t_i are obtained for each building i. To maximize the fidelity of the approximation, a dynamic constraint-only virtual battery is chosen as a prototype polytope expressed as follows:

$$\mathcal{P}_0 := \left\{ x \in \mathbb{R}^{N_f} \;\middle|\; \begin{array}{c} y(t+1) = ay(t) + x(t) \\ \underline{y}(t+1) \leq y(t+1) \leq \overline{y}(t+1) \end{array} \right\} \tag{19}$$

Where x is the state of the charge or discharge power of the battery, y is the battery state, and a the dissipation rate of the battery. In H-polytopic form :

$$\mathcal{P}_0 := \left\{ x \in \mathbb{R}^{N_f} \mid H_0 x \leq d_0 \right\} \tag{20}$$

$$H_0 = [-M_0; M_0] \in \mathbb{R}^{2N_f \times N_f}, d_0 \in \mathbb{R}^{2N_f} \tag{21}$$

$$M_0 = \begin{pmatrix} a & 0 & \dots & 0 \\ a^2 & a & \ddots & \vdots \\ \vdots & \vdots & \ddots & 0 \\ a^{N_f-1} & a^{N_f-2} & \dots & a \end{pmatrix} \tag{22}$$

As expressed in (Zhao et al., 2017), the optimal inner approximation of $\mathcal{P}_i^{rl,th}$ is given by $\beta_i^* = 1/s_i^*$ and $t_i^* = -r_i^*/s_i^*$ where r_i^* and s_i^* are optimal solutions of the following problem :

$$\begin{aligned} \min_{s_i, G, r_i} \quad & s_i \\ \text{s.t.} \quad & GH_0 = \hat{d}_i^{rl,th} \\ & Gd_0 \leq s_i \hat{H}_i^{rl,th} + \hat{d}_i^{rl,th} r_i \\ & H_0 r_i \leq d_0 \\ & G_{i,j} \geq 0, s_i > 0 \end{aligned} \tag{23}$$

The constraint $H_0 r_i \leq d_0$ ensures that the point (0,0) is included in the approximate polytope, allowing the building to not offer flexibility and not make the only choice to offer flexibility.

Finally, the approximation of the flexibility capacity polytope is given by the set of optimal factors β_i^* and t_i^*:

$$\mathcal{P}_i^{ap} = \mathcal{P}_i^{ap,pw} \cap (\beta_i^* \mathcal{P}_0 + t_i^*) \tag{24}$$

An example of an approximation is given in figure 5.

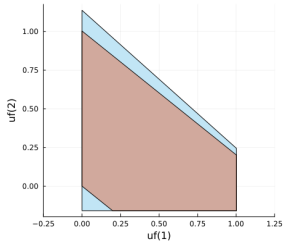

Fig. 5. Approximation polytope $\mathcal{P}_i^{ap}$ (light red) of the capacity polytope $\mathcal{P}_i^{rl}$ (light blue)

2.3 Aggregation of flexibility

The exact aggregated flexibility capacity of all buildings is obtained by the Minkowski Sum $\mathcal{P}_{MS}$ of the individual flexibilities :

$$\mathcal{P}_{MS} = \oplus_j \mathcal{P}_j = \left\{ \mathbf{P}_{MS}(k) \in \mathbb{R}^{N_f} \;\middle|\; \begin{array}{c} \mathbf{P}_{MS}(k) = \sum_j \mathbf{P}_j(k), \\ \mathbf{P}_j(k) \in \mathcal{P}_j \end{array} \right\} \tag{25}$$

As the exact calculation of the MS is complex and time-consuming, an approximation of the MS is needed. As discussed in the introduction, aggregation of homothet approximations (Zhao et al., 2017) is easy to compute. Also, for the power-only approximate polytope, the sum is also easy to compute, as it is a sum of n-dimension parallelotope. Therefore, in our case, we propose an approximation of the MS that consists of doing side by side the sum of each power approximation and thermal approximation. This proposition is more efficient for computation time of the flexibility capacity aggregation.

First, the sum of the power polytope, based on their form, can be written as :

$$\oplus_i \mathcal{P}_i^{ap,pw} := \left\{ u_f \in \mathbb{R}^{N_f} \;\middle|\; H^{rl,pw} u_f \leq \sum_{i=1}^{N} d_i^{ap,pw} \right\} \tag{26}$$

Then, as expressed in (Zhao et al., 2017), the MS of homothet polytopes of the same prototypes, knowing each scaling and translation factor, can be expressed by :

$$\oplus_i (\beta_i^* \mathcal{P}_0 + t_i^*) = \sum_i \beta_i^* \mathcal{P}_0 + \sum_i t_i^* \tag{27}$$

Then, the approximation of the MS $\mathcal{P}_{ag}^{ap}$ can be derived from the intersection of the sums of each set of constraints:

$$\mathcal{P}_{ag}^{ap} = (\oplus_i \mathcal{P}_i^{ap,pw}) \cap (\oplus_i (\beta_i^* \mathcal{P}_0 + t_i^*)) \tag{28}$$

However, this approximation is not always included in the real MS, as the intersection of sums is not always included in the sum of intersections, which can be a problem in a disaggregation phase. The limitation step described in equation (18) aims to minimize the difference between the sum of intersections and the intersection of sums. In addition, to guarantee disaggregation, a slack variable will be introduced during this phase and will be described in section 3.

3. CASE STUDY

3.1 Implementation

After developing our methodology of MS approximation, we now aim to implement it in a microgrid control optimization problem. Our microgrid will be composed of a battery (BT), solar panels (PV), dispatchable generator (DG) and the load composed of a population of N buildings. The microgrid control optimization problem is formulated as MILP problem; the objective is to minimize the load shedding and the curtailment of RES by optimizing energy flows (microgrid unit commitment, flexibility decisions...). In case of global flexibility decision, a phase of disaggregation is needed to share the decision among all buildings. This phase is made through a simple equal-sharing strategy, such as :

$$\begin{aligned} \min_{\{\mathbf{u}_f\}_{i\in\mathcal{N}}} \quad & \sum_{i=1}^{N} \left\| \mathbf{u}_{f,i} - \frac{\mathbf{u}_f^*}{N} \right\|_1 + c_\varepsilon \|\varepsilon_{dis}\|_1 \\ \text{s.t.} \quad & \mathbf{u}_{f,i} \in \mathcal{P}_i^{ap}, \quad \varepsilon_{dis} \in \mathbb{R}^{N_f} \\ & \mathbf{u}_f^* = \sum_{i\in\mathcal{N}} \mathbf{u}_{f,i} + \varepsilon_{dis} \end{aligned} \tag{29}$$

With $\mathcal{N}$ the set of buildings, $\mathbf{u}_f^*$ the global flexibility decision obtain at microgrid control optimization problem, $\mathbf{u}_{f,i}$ the individual flexibility decision of the building i, ε_{dis} the slack variable implemented to ensure the feasibility of disaggregation and c_ε the weight on the slack variable. A similar problem is set to distribute equally the baseline power remaining in case of presence of shedded power.

3.2 comparison of approximation approaches

First, we need to compare our methodology to other approximation methods in terms of approximation fidelity and computation time to validate it. We will consider a virtual battery approximation method (Zhang and Guéguen, 2024) and a classic homothet battery approximation method (Zhao et al., 2017). For this purpose, we consider two residential buildings with the same temperature comfort habits. The sample time Δt is set to one hour but can be set to shorter sample times (30 or 15 min for example). We use as a prototype polytope a dynamic constraints-only virtual battery of dissipation rate $a = 0.8$ with d_0 defined as a unit vector for the thermal constraints-only polytope approximation. The simulation is made during a period of 48h. The outside temperature θ_{ext} and the irradiance I_{PV} came from historical data of 2019 in Rennes, France, using *renewable.ninja* (Staffell and Pfenninger, 2016).

The microgrid is set with a BT of 5 kWh of capacity, the DG can go from 0.5 kW to 5kW and a rated power of PV of 16 kW peak. For the homothet method, we will consider a regular parallelotope where each value of the matrix d are equals (a square in dimension 2), that allow to cover all situations.

To evaluate the fidelity of each approximation, we use the normalized volume ratio for each building at each time step. This ratio is expressed as :

$$r_{vol} = \sqrt[N_f]{vol(\mathcal{P}_i^{ap})/vol(\mathcal{P}_i^{rl})} \tag{30}$$

3.3 scaling comparison

We consider 100 different types of users for the thermal behavior, such as :

- a residential building with working hours outside the house (50 buildings)
- a residential building with full-time occupation (25 buildings)
- a company building used only during work hours (25 buildings)

The microgrid sizing is updated to fit the increased number of consumers. The battery size is set to 75 kWh of energy capacity, 60 kW of maximum power of DG and 600 kW peak of solar panels. We will use the same settings for the homothet characteristics, the sample time is set to one hour, and we will simulate during a winter period of 100 days for a total of 2400 instant of simulation.

As discussed in the method section, the global flexibility decision may be not disaggregate totally. Therefore, for this scaling comparison, the remaining power during disaggregation phase extracted from the slack variable ε_{dis} will be measured for different scenarios :

- Scenario 1 : each type of consumer will have the same thermal routine and the same thermal building characteristics
- Scenario 2 : different thermal routine but same thermal building characteristics
- Scenario 3 : same thermal routine but different thermal building characteristics
- Scenario 4 : Different thermal routine and different thermal building characteristics

Optimizations are made with Gurobi (Gurobi Optimization, LLC, 2024) and JuMP (Lubin et al., 2023) through the Julia programming language (Bezanson et al., 2015). The computer used to do the simulations is equipped with an Intel Core Ultra 7 165H 3.80 GHz CPU with 32 GB of RAM. At each time step, we use multi-threading as parallel computing for each building individual calculus (baseline, polytope approximation and thermal simulation) to limit the computation time. The number of threads of execution is set to 22 based on the processor.

4. RESULTS

4.1 comparison of approximation approaches results

The figure 6 shows the mean value of all volume ratios evaluated all over the simulation for each approximation method. The limit of N_f is set to 7 because, for higher values, the EMS will have enough vision to operate efficiently without flexibility. We can observe for the VB approach that we stop measuring for high values of N_f because the individual approximation or the MS approximation may not find a solution in an acceptable time, which can't be integrated in a microgrid control optimization problem. As expected, the VB approximation is still the best approximation method in terms of fidelity, but as shown in figure 7, the computation time is growing exponentially with the flexibility horizon, while our method is as fast as the homothet approximation and still validates a good level of approximation.

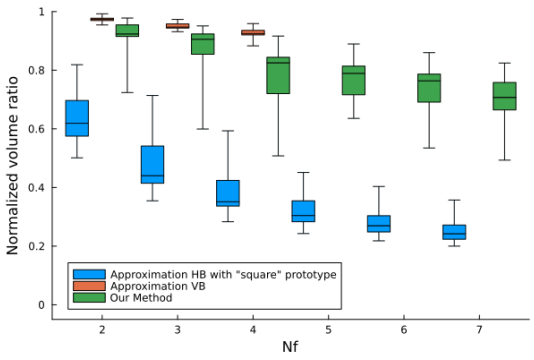

Fig. 6. Volume ratio of all buildings according to Nf

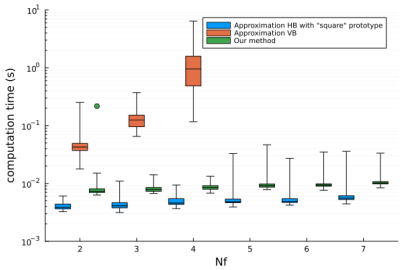

Fig. 7. Computation time for all buildings according to Nf

4.2 scaling comparison results

For the scaling comparison, the figure 8 shows the rate of time when there is power remaining from the disaggregation step for different values of N_f. We can observe that, for each scenario, we have remaining power among the 2400 instants less than 0.5% of the time. For all those cases, the mean ratio of remaining power is around 5% (5kW remain from around 100kW of decision). However, we can observe two instant where 15% (15 kW) of the global decision remains to be shared. In the considered case, as the only remaining power flexibility is from upward global flexibility decision, the remaining power goes into curtailment. In case of downward flexibility, shedding would be generated.

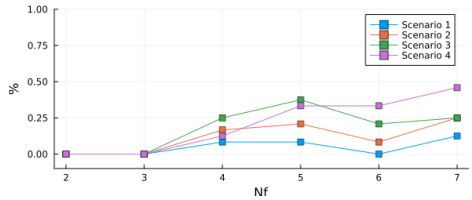

Fig. 8. Percentage of time when the global flexibility decision is not fully disaggregated according to Nf

5. CONCLUSION

In this paper, a method for flexibility approximation and aggregation for microgrid control applications has been developed. This method has been implemented for a large population of buildings in a long scenario. The results show that our method, compared to others, validates a trade-off between fidelity of approximation and computation time. However, with a population of 100 buildings, we can have a few moments when we have remaining power after the disaggregation phase but with small values. A perspective of work is to address the remaining power non-disaggregate to elements of our microgrid. Also, an investigation of the flexibility interests compared to an optimized control over a long horizon must be done. Another perspective is to add comfort criteria to the flexibility capacity to avoid, in some cases, an overuse of flexibility, which could lead to non-comfortable living households. In future work, unshared flexibility will be considered as an economic penalization for the aggregator and taken into account for the sizing optimization problem.

REFERENCES

Barot, S. (2017). *Aggregate load modeling for Demand Response via the Minkowski sum.* Ph.D. thesis, New Jersey Institute of Technology.

Bezanson, J., Edelman, A., Karpinski, S., and Shah, V.B. (2015). Julia: A Fresh Approach to Numerical Computing. doi:10.48550/arXiv.1411.1607. ArXiv:1411.1607 [cs].

Boodi, A., Beddiar, K., Amirat, Y., and Benbouzid, M. (2022). Building Thermal-Network Models: A Comparative Analysis, Recommendations, and Perspectives. *Energies*, 15(4), 1328. doi:10.3390/en15041328.

Essayeh, C. and Morstyn, T. (2023). Optimal sizing for microgrids integrating distributed flexibility with the Perth West smart city as a case study. *Applied Energy*, 336, 120846. doi:10.1016/j.apenergy.2023.120846.

Gurobi Optimization, LLC (2024). Gurobi Optimizer Reference Manual.

Lubin, M., Dowson, O., Garcia, J.D., Huchette, J., Legat, B., and Vielma, J.P. (2023). JuMP 1.0: Recent improvements to a modeling language for mathematical optimization. doi:10.48550/arXiv.2206.03866. ArXiv:2206.03866 [cs].

Lund, P.D., Lindgren, J., Mikkola, J., and Salpakari, J. (2015). Review of energy system flexibility measures to enable high levels of variable renewable electricity. *Renewable and Sustainable Energy Reviews*, 45, 785–807. doi:10.1016/j.rser.2015.01.057.

Müller, F.L., Szabó, J., Sundström, O., and Lygeros, J. (2019). Aggregation and Disaggregation of Energetic Flexibility From Distributed Energy Resources. *IEEE Transactions on Smart Grid*, 10(2), 1205–1214. doi:10.1109/TSG.2017.2761439.

Nazir, M.S., Hiskens, I.A., Bernstein, A., and Dall'Anese, E. (2018). Inner approximation of minkowski sums: A union-based approach and applications to aggregated energy resources. In *2018 IEEE Conference on Decision and Control (CDC)*, 5708–5715. doi:10.1109/CDC.2018.8618731.

Saavedra, A., Negrete-Pincetic, M., Rodriguez, R., Salgado, M., and Lorca, A. (2022). Flexible load management using flexibility bands. *Applied Energy*, 317, 119077. doi:10.1016/j.apenergy.2022.119077.

Staffell, I. and Pfenninger, S. (2016). Using bias-corrected reanalysis to simulate current and future wind power output. *Energy*, 114, 1224–1239. doi:10.1016/j.energy.2016.08.068.

Zhang, Z. and Guéguen, H. (2022). Bilevel Optimization Based on Building Dynamic Flexibility Capacity in Microgrid. *IFAC-PapersOnLine*, 55(9), 274–279. doi:10.1016/j.ifacol.2022.07.048.

Zhang, Z. and Guéguen, H. (2024). Aggregation of building predictive energy flexibility in smart microgrid. *International Journal of Electrical Power & Energy Systems*, 160, 110073. doi:10.1016/j.ijepes.2024.110073.

Zhao, L., Zhang, W., Hao, H., and Kalsi, K. (2017). A Geometric Approach to Aggregate Flexibility Modeling of Thermostatically Controlled Loads. *IEEE Transactions on Power Systems*, 32(6), 4721–4731. doi:10.1109/TPWRS.2017.2674699.

Öztürk, E., Rheinberger, K., Faulwasser, T., Worthmann, K., and Preißinger, M. (2022). Aggregation of Demand-Side Flexibilities: A Comparative Study of Approximation Algorithms. *Energies*, 15(7), 2501. doi:10.3390/en15072501.